

Signature of Quantum Chaos in SQUID's

Takeo Kato *, Ken-ichi Tanimoto, Katsuhiro Nakamura

*Department of Applied Physics, Osaka City University, Sumiyoshi-ku, Osaka
558-8585, Japan*

Abstract

Spectral statistics in band structures is studied in a realistic model describing superconducting quantum interference devices (SQUID's). By controlling an external magnetic flux, the level statistics may show a crossover from the GUE to the GOE. Effects of secondary discrete symmetries seen in specific regions of the first Brillouin zone are also discussed.

Key words: SQUID; Quantum chaos; Band structure

PACS: 05.45.Mt, 74.50.+r, 83.25.Na

Recent development in physics of quantum chaos has its origin in studies of spectral statistics of quantum systems whose corresponding classical dynamics exhibits chaos. It is now well known that statistical properties of energy spectra are universal in various quantum systems including, e.g., atoms, nuclei, and electron billiards as well as classical wave-mechanical systems such as microwave cavities [1]. Recently, spectral statistics in band structures in extended periodic systems has been studied for driven systems [2], electronic systems [3,4,5,6] and photonic crystals [7]. Band structures have also been studied in the context of avoided band crossings [8]. Most of these band-structured systems, however, are sensitive to the accompanying impurities and/or inhomogeneity. It is highly desirable to find corresponding systems robust against the extrinsic randomness.

In this Letter, we consider superconducting quantum interference devices (SQUID's), whose periodic features are described by a few macroscopic variables called superconducting phases. We here focus on small SQUID's with three junctions where a two-dimensional periodic potential for the phases can be realized. Because of the macroscopic nature of the phases, the potential is robust against impurities and/or inhomogeneities of the system. This feature

* Corresponding author.

Email address: kato@a-phys.eng.osaka-cu.ac.jp (Takeo Kato).

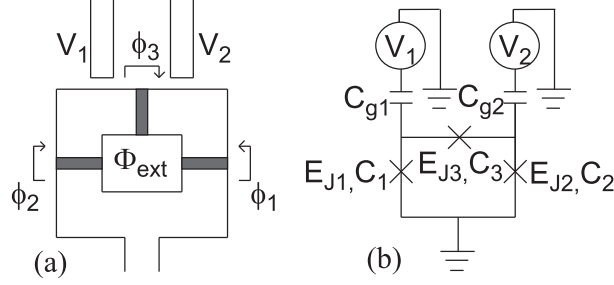


Fig. 1. (a) The three-junction system considered in this Letter. The states of the SQUID are controlled by a magnetic flux Φ_{ext} and gate voltages, V_i 's. The flux is vertical to the page. (b) The equivalent circuit of the SQUID. The Josephson energy and capacitance of the i -th junction (shown by \times) are denoted by E_{Ji} and C_i , respectively. The two upper superconducting islands are coupled to the voltage gates through capacitances, C_{g1} and C_{g2} , respectively.

is of great advantage to study the spectral statistics; This is particularly in contrast to the two-dimensional electron systems where impurity scattering and inhomogeneity are unavoidable. The SQUID system also has the advantage of controllability. Potential shapes for the phases can be controlled by an external magnetic flux, and the Bloch wave-numbers can be chosen by voltage gates. In the limited context of application to quantum computations, one is concerned only with the lowest few quantum levels [10,11,12,13]. Moreover generally, however, if level spectroscopy at a high-energy region will become possible, this system would give a good stage for studies of quantum chaos in band structures.

Already we investigated the classical phase dynamics of SQUID's with two junctions and discovered the mysterious normal diffusion phenomena there: The diffusion coefficient was found to take a fractal-like feature [14]. SQUID's with two junctions, however, were on scale of $100\mu\text{m}$ and thereby classical. On the contrary, SQUID's with three junctions considered in this Letter is on scale of $1\mu\text{m}$ and their quantization is highly desirable to elucidate a quantum signature of the underlying mysterious normal diffusion phenomena.

The configuration of the SQUID system is shown in Fig. 1 (a), while the equivalent circuit is shown in Fig. 1 (b). The loop of superconductor includes three Josephson junctions denoted with \times in the circuit. The Josephson energy and capacitance of the i -th junction are denoted with E_{Ji} and C_i , respectively. The two upper superconducting islands are coupled to the voltage gates through the capacitances, C_{g1} and C_{g2} , respectively. The states of this SQUID are controlled by an external flux penetrating through the loop, Φ_{ext} and by gate voltages, V_i 's.

By controlling fabrication conditions, both the Josephson energies and capacitances can be varied. In this Letter, for simplicity we assume $E_{J1} = E_{J2} = E_{J3}(\equiv E_J)$. We also assume $C_1, C_2, C_3 \ll C_{g1} = C_{g2}(\equiv C_g)$, where the junc-

tion capacitances can be neglected. These assumptions are not essential to the discussion of the classical-quantum correspondence through spectral statistics. We assume these conditions because it is convenient to study effects of discrete symmetries such as parity.

Behaviors of the Josephson junction are described by the superconducting phase difference at the junction. We denote the phase difference at each junction with ϕ_i . The directions to define these differences are shown by the arrows in Fig. 1 (a). Then, the Hamiltonian of this SQUID consists of three parts:

$$H = H_C + H_J + H_L, \quad (1)$$

where H_C , H_J and H_L are a charging energy, a junction energy and an inductance energy, respectively. First, we show that the latter two parts correspond to a potential energy for the phase differences. The junction energy is determined by the phase differences as

$$H_J = -E_J \cos \phi_1 - E_J \cos \phi_2 - E_J \cos \phi_3, \quad (2)$$

while the inductance energy is determined by the persistent current along the loop, and given as

$$H_L = \frac{\Phi_0^2}{2L} \left(\phi_1 - \phi_2 - \phi_3 - 2\pi \frac{\Phi_{\text{ext}}}{\Phi_0} \right)^2. \quad (3)$$

Here, $\Phi_0 = h/2e$ is a unit flux, and L is an inductance determined by the size and shape of the loop. Here, we consider a small loop with a small inductance satisfying $\Phi_0^2/2L \gg E_J$. Such SQUID can be easily realized experimentally by fabricating the superconducting loop with the size of order of micrometers. In this small SQUID, the inductance energy approximately gives a constraint $\phi_1 - \phi_2 - \phi_3 - 2\pi\Phi_{\text{ext}}/\Phi_0 = 0$ on the phases. By using this constraint, the potential energy for the phases are obtained as

$$H_J = -E_J \cos \phi_1 - E_J \cos \phi_2 - E_J \cos(\phi_1 - \phi_2 - 2\pi f), \quad (4)$$

where $f = \Phi_{\text{ext}}/\Phi_0$ is a normalized external flux. This two-dimensional periodic potential has a square unit cell defined by $0 \leq \phi_1 \leq 2\pi$ and $0 \leq \phi_2 \leq 2\pi$.

On the other hand, the charging energy H_C is described by the charges of the junctions. We denote the charge induced at the i -th gate capacitance by $Q_i = -2en_i$, where n_i is the number of the induced Cooper-pair. It is known that the number of the Cooper pairs, n_i is conjugate to the phase difference

ϕ_i and the following exchange relation satisfies:

$$[\phi_i, n_j] = i\delta_{ij}, \quad (1 \leq i, j \leq 2). \quad (5)$$

Since the junction capacitances are neglected, the charging energy is calculated as [10]

$$H_C = \frac{1}{2C_g}(Q_1^2 + Q_2^2) + V_1Q_1 + V_2Q_2. \quad (6)$$

This energy is rewritten by using the numbers of Cooper-pairs as

$$H_C = 4E_C(n_1 - n_1^*)^2 + 4E_C(n_2 - n_2^*)^2, \quad (7)$$

where $E_C = e^2/2C_g$, and $n_i^* = C_g V_i/2e$ is a normalized gate voltage. This gives a kinetic energy for the phases.

Here, note that the gate voltages can control the Bloch wave-numbers. This can be checked by considering the wave function $\Psi(\phi_1, \phi_2)$ satisfying the periodic condition for both ϕ_1 and ϕ_2 . For the alternative wave function $\xi(\phi_1, \phi_2)$ defined by $\Psi(\phi_1, \phi_2) = e^{-in_1^*\phi_1 - in_2^*\phi_2}\xi(\phi_1, \phi_2)$, the kinetic part of the Hamiltonian for $\xi(\phi_1, \phi_2)$ is modified as

$$\tilde{H}_C = 4E_C n_1^2 + 4E_C n_2^2, \quad (8)$$

while the wave function $\xi(\phi_1, \phi_2)$ satisfies the following Bloch theorem

$$\xi(\phi_1 + 2\pi m_1, \phi_2 + 2\pi m_2) = e^{im_1 n_1^* + im_2 n_2^*} \xi(\phi_1, \phi_2). \quad (9)$$

Hence, the normalized voltages, n_i^* 's correspond to the Bloch wave-numbers for the Hamiltonian $\tilde{H} = \tilde{H}_C + H_J$. We find that the feature of classical phase dynamics for \tilde{H} leads to the same mysterious normal diffusion phenomena in SQUID's with two junctions [14]. (We suppress the classical result in this Letter.)

The energy spectrum of the SQUID is obtained by diagonalizing the Hamiltonian $H = H_C + H_J$ for fixed values of n_1^* and n_2^* . We adopt the charge eigenstates as the base wavefunctions. Then, it is convenient to rewrite the Hamiltonian by introducing an annihilation operator $b_i = e^{i\phi_i}$ satisfying an exchange relation $[n_i, b_j] = -b_i\delta_{ij}$ as

$$H = 4E_C(n_1 - n_1^*)^2 + 4E_C(n_2 - n_2^*)^2 - \frac{E_J}{2}(b_1 + b_1^\dagger) - \frac{E_J}{2}(b_2 + b_2^\dagger) - \frac{E_J}{2}(b_1 b_2^\dagger e^{-2\pi i f} + b_2 b_1^\dagger e^{2\pi i f}). \quad (10)$$

The charging energy gives diagonal parts, while the junction energy off-diagonal parts. Here, we should note that if f is an integer or half-integer, the Hamiltonian can be represented by a real matrix.

In this Letter, we take $E_C = 0.002E_J$, and consider the case of $f = 0.5$ and $f = 0.25$. The classical phase dynamics based on Eq. (1) shows chaotic behaviors in the dominant region of the corresponding Poincare section, when the energy is taken between the saddle-point potential energy E_{sad} and the potential-top energy E_{top} . Here, the spectral properties are studied in the range $E_{\text{sad}} \leq E \leq E_{\text{sad}} + 0.75(E_{\text{top}} - E_{\text{sad}})$. The ordinary unfolding procedure is performed to obtain the level statistics [15,16]. Depending on the Bloch wave-numbers, n_1^* and n_2^* , the energy spectra show various statistics: the Poisson-like, GOE, and GUE statistics. To see this wave-number dependence, we fit the spectra to the Izrailev distribution [17]

$$P(S) = A \left(\frac{\pi S}{2} \right)^\beta \exp \left[-\frac{1}{16} \beta \pi^2 S^2 - \left(B - \frac{1}{4} \pi \beta \right) S \right], \quad (11)$$

which interpolates among different universality classes by the parameter β . The parameters, A and B are normalization constants. One can recover the Poisson distribution for $\beta = 0$, while it agrees with the GOE (GUE) distribution for $\beta = 1$ ($\beta = 2$) on the 5 percent level. Although the Izrailev distribution is originally proposed for localization problems, we here use it for qualitative characterization of the spectra.

The density plots of the fitted values of β in the first Brillouin zone (FBZ) of the n_1^* - n_2^* plane are shown in Fig. 2. In the case of $f = 0.25$, the spectra shows the GUE distribution ($\beta = 2$) except for the symmetry lines, $n_1^* = n_2^*$ and $n_1^* = -n_2^*$, and the points, $(n_1^*, n_2^*) = (\pm 0.5, 0)$ and $(0, \pm 0.5)$. In the case of $f = 0.5$, the spectra shows the GOE distribution ($\beta = 1$) except the same symmetry lines and points. Let us first discuss the universality class of the region, which is on neither the symmetry lines nor points. In the case of $f = 0.25$, the Hamiltonian includes the imaginary number in the last term in (10). Hence, it is expected that the time-reversal symmetry is broken, and the level statistics is governed by the GUE. Actually, the nearest neighbor distribution $P(S)$ and spectral rigidity $\Delta_3(L)$ agree well with the GUE statistics as shown in Fig. 3. In the case $f = 0.5$, the Hamiltonian can be expressed by a real symmetric matrix as seen in (10). Hence, the system exhibits the time-reversal symmetry, and the level statistics belongs to the GOE. Actually, the result for $P(S)$ and $\Delta_3(L)$ agrees with the GOE statistics as shown in Fig. 4. Since the value of f can be varied by the external magnetic flux, the universality class can be easily controlled in this SQUID system.

Thus, the signature of quantum chaos has been obtained in the SQUID system. So, the main purpose of this Letter has been achieved. It, however, remains

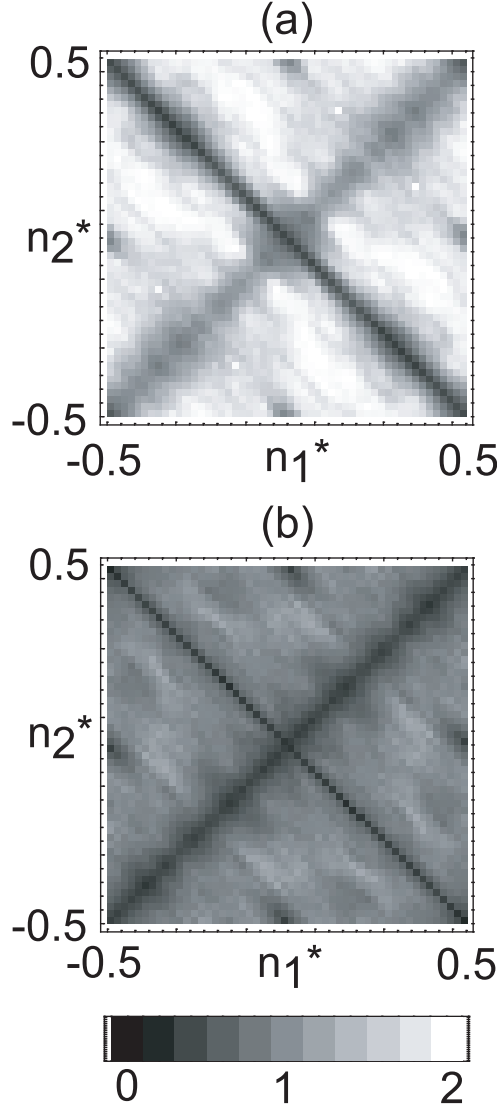


Fig. 2. The density plot of the parameter β obtained by fitting the spectrum to the Izrailev distribution: (a) $f = 0.25$ and (b) $f = 0.5$. $\beta = 0$ (the darkest) and $\beta = 2$ (the brightest).

to explain the deviations from the expected universal class on the symmetry lines and points as seen in Fig. 2. We end this Letter by brief discussion on this secondary feature in the SQUID system.

First, we consider the case of $f = 0.25$. We divide the regions where the deviation from the GUE statistics is seen into five parts: (A) the line $n_1^* = n_2^*$ ($n_1^* \neq 0$), (B) the line $n_1^* = -n_2^*$ ($n_1^* \neq 0$), (C) the point $(n_1^*, n_2^*) = (0, 0)$, (D) the points $(n_1^*, n_2^*) = (\pm 0.5, 0)$, and (E) the points $(n_1^*, n_2^*) = (0, \pm 0.5)$. The deviation from the GUE statistics in each region can be explained by corresponding additional symmetries characterized by operators commuting with the Hamiltonian. In the region (A), it is crucial to consider the operator P_1

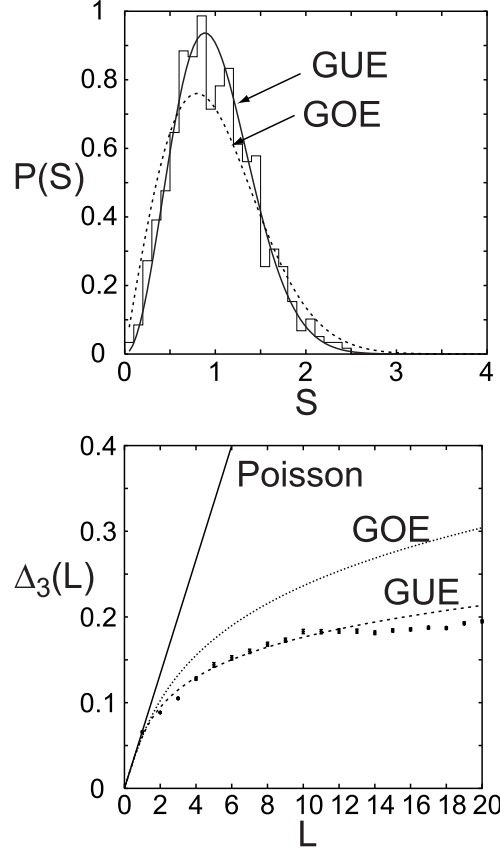


Fig. 3. (a) The nearest-neighbor level distribution $P(S)$ and (b) the spectral rigidity $\Delta_3(L)$ for $f = 0.25$. The normalized gate voltages are taken as $(n_1^*, n_2^*) = (0.25, 0)$.

defined by $|n_2, n_1\rangle = P_1|n_1, n_2\rangle$, where $|n_1, n_2\rangle$ is the eigenkets of the Cooper-pair-number operator. It can be checked that the operator P_1T commutes with the Hamiltonian on the line $n_1^* = n_2^*$, where T is the time-reversal operator. Then, the spectral statistics is governed by the GOE statistics by the discussion of the false time-reversal symmetry [18]. Similarly, in the region (B), the mirror-reversal operator P_2 defined by $|-n_2, -n_1\rangle = P_2|n_1, n_2\rangle$ commutes with the Hamiltonian. Then, the eigenkets can be classified into two kinds by the parity defined as the eigenvalue of the operator P_2 . The spectrum taken only for even(odd) states is expected to show the level repulsion. The level correlation between odd and even states is, however, suppressed because the matrix elements of the Hamiltonian $\langle\psi_i|H|\psi_j\rangle$ is zero when ψ_i and ψ_j have different parity. As a result, the spectrum become the mixture of two independent GUE statistics. This mixed level statistics is denoted in this Letter with 2-GUE [5,6]. In the region (C), both P_1T and P_2 commutes with the Hamiltonian. Then, the spectrum becomes the mixture of the two independent GOE statistics (2-GOE). In the region (D), a kind of the mirror reversal symmetries exists. The symmetry operator P_3 is defined as $|1 - n_1, -n_2\rangle = P_3|n_1, n_2\rangle$, and P_3T commutes with the Hamiltonian. Then, the spectral statistics obeys the GOE by the same reason as the region (A). Similarly, in the region (E), P_4T com-

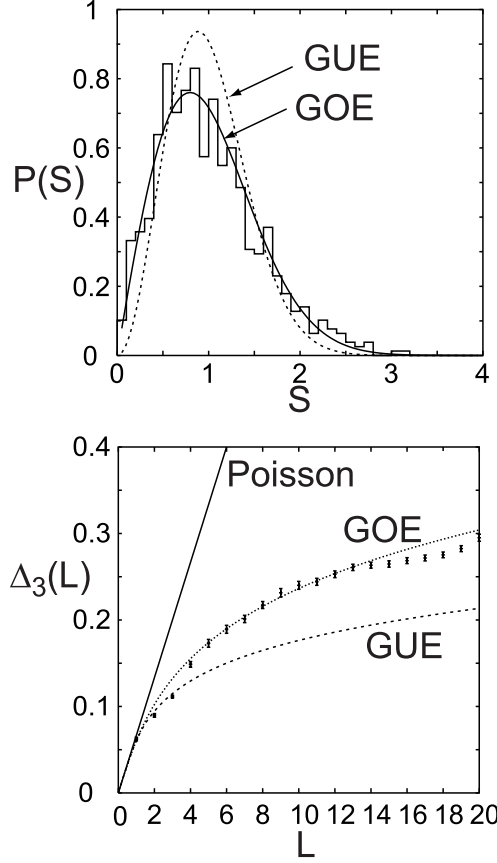


Fig. 4. (a) The nearest-neighbor level distribution $P(S)$ and (b) the spectral rigidity $\Delta_3(L)$ for $f = 0.5$. The normalized gate voltages are taken as $(n_1^*, n_2^*) = (0.25, 0)$.

mates with the Hamiltonian, where P_4 is defined as $|-n_1, 1 - n_2\rangle = P_4|n_1, n_2\rangle$. Hence, the level statistics is described by the GOE.

Next, we consider the case of $f = 0.5$. The deviation from the GOE statistics is observed near the same lines and points as the case of $f = 0.25$. The explanation of this deviation is quite parallel to the previous paragraph. In the region (A) and (B), the operator P_1 and P_2 commute with the Hamiltonian, respectively. Hence in these regions, the level spectrum becomes the mixture of two independent GOE statistics (2-GOE). In the region (C), because both P_1 and P_2 commute with the Hamiltonian, the spectrum obeys the 4-GOE statistics. In the region (D) and (E), the spectrum is described by the 2-GOE statistics, since P_3 and P_4 commute with the Hamiltonian, respectively.

In summary, spectral statistics in band structures has been discussed in a realistic SQUID model. This system can change the Bloch wave-numbers by controlling the gate voltages. The normalized external flux f can control the time-reversal symmetry of the system, and the crossover from the GUE to the GOE can be observed by varying f . By taking the circuit parameters as symmetric, the effect of the secondary discrete symmetries can also be dis-

cussed. On specific lines and points in the first Brillouin zone, the spectra may obey different statistics determined by the operator characterizing the discrete symmetry of the system. We expect that this work can be a starting point to consider the quantum chaos in a well-controlled system. A variety of dynamical features of quantum chaos can also be observed in the quantum dynamics by using the excellent ability of quantum manipulation and measurement in the SQUID system, which will be investigated in due course.

The authors thank A. Terai for useful discussion and critical reading of the manuscript.

References

- [1] H.-J. Stöckmann, Quantum Chaos an introduction, Cambridge University Press, Cambridge, 1999.
- [2] S. Miyazaki, A. R. Kolovsky, Phys. Rev. E 50 (1994) 910.
- [3] E. R. Mucciolo, R. B. Capaz, B. L. Altshuler, J. D. Joannopoulos, Phys. Rev. B 50 (1994) 8245.
- [4] H. Silberbauer, P. Rotter, U. Rössler, M. Suhrke, Europhys. Lett. 31 (1995) 393.
- [5] Hongqi Xu, J. Phys. Condens. Matter 10 (1998) 4001.
- [6] Hongqi Xu, B.-Y. Gu, J. Phys. Condens. Matter 13 (2001) 9505.
- [7] L. N. Gumen, J. Arriagab, A. A. Krokhinb, Physica E 13 (2002) 459.
- [8] R. Ketzmerick, K. Kruse, D. Springsguth, T. Geisel, Phys. Rev. Lett. 84 (2000) 2929.
- [9] A. Barone, G. Paterno, Physics and Application of the Josephson Effect, Wiley-Interscience, New York, 1982.
- [10] T. P. Orlando, J. E. Mooij, L. Tian, C. H. van der Wal, L. Levitov, S. Lloyd, J. J. Mazo, Phys. Rev. B 60 (1999) 15398.
- [11] Yu. Makhlin, S. Schön, A. Shnirman: Rev. Mod. Phys. 73 (2001) 357.
- [12] Casper H. van der Wal, A. C. J. ter Haar, F. K. Wilhelm, R. N. Schouten, C. J. P. M. Harmans, T. P. Orlando, S. Lloyd, J. E. Mooij, Science 290 (2000) 773.
- [13] I. Chiorescu, Y. Nakamura, C. J. P. M. Harmans, J. E. Mooij, Science 299 (2003) 1869.
- [14] K. Tanimoto, T. Kato, K. Nakamura, Phys. Rev. B 66 (2002) 012507.
- [15] F. Haake, Quantum Signatures of Chaos, 2nd ed., Springer-Verlag, Berlin, 2000.

- [16] M. L. Mehta, Random Matrices, 2nd ed., Academic Press, San Diego, CA, 1991.
- [17] F. M. Izrailev, Phys. Lett. A 134 (1998) 13.
- [18] M. Robnik, M. V. Berry, J. Phys. A 19 (1986) 669.